

GENERATION OF LOW FREQUENCY ELECTROMAGNETIC WAVE BY INJECTION OF COLD ELECTRON FOR RELATIVISTIC AND NON-RELATIVISTIC SUBTRACTED BI-MAXWELLIAN DISTRIBUTION WITH PERPENDICULAR AC ELECTRIC FIELD FOR MAGNETOSPHERE OF URANUS

R. S. Pandey* and R. Kaur

Department of Applied Physics, Amity Institute of Applied Sciences, Amity University, Noida, U.P, India

Abstract—Effect of cold electron beam for Whistler mode waves have been studied for relativistic and non-relativistic subtracted bi-Maxwellian distribution in the presence of perpendicular AC electric field to magnetic field by using the method of characteristic solutions and kinetic approach. The detailed derivation and calculations has been done for dispersion relation and growth rate for magnetosphere of Uranus. Parametric analysis has been done by changing plasma parameters: thermal velocity, ac frequency, temperature anisotropy, etc.. The effect of AC frequency on the Doppler shifting frequency and comparative study of relativistic and non-relativistic effect on growth rate are analyzed. The new results using subtracted bi-Maxwellian distribution function are found and discussed in relation to a bi-Maxwellian distribution function. It is seen that the effective parameters for the generation of Whistler mode wave are not only the temperature anisotropy but also the relativistic factor, AC field frequency, amplitude of subtracted distribution and width of the loss-cone distribution function which has been discussed in result and discussion section.

1. INTRODUCTION

The Voyager 2 encounter of Uranus in January 1986 provided the opportunity to observe yet another planetary magnetosphere and compare the plasma physical processes taking place there, to those

Received 18 September 2012, Accepted 22 October 2012, Scheduled 3 November 2012

* Corresponding author: Rama Shankar Pandey (pandeyramashankar@yahoo.com).

occurring in magnetosphere of Earth, Jupiter and Saturn [1]. The presence of magnetic field at Uranus was not known until the Voyager's arrival. This offered a rich environment for the study of magnetospheric interactions. In addition to standard array of magnetosphere phenomena, ranging from upstream ion events to the bow shock and magnetospheric boundary structures, from an intense inner region of hard particles radiation, to a soft magneto tail plasma sheet, the magnetosphere of Uranus presents an unusual configuration with unique characteristics.

Observations revealed strong electromagnetic and electrostatic plasma turbulence and whistler mode emissions (chorus and hiss) in the inner magnetosphere of Uranus. It is known that whistler-mode waves are electromagnetic waves that propagate through the magnetosphere along the ambient magnetic field (as anisotropy in plasma is introduced by magnetic field) at frequencies below electron-cyclotron frequency and electron plasma frequency. Kurth [2] discussed how whistler mode emissions play a critical role in the dynamics of Uranian magnetosphere by controlling pitch angle scattering and loss of magnetically trapped radiation belt particles. Whistler mode instability in magnetosphere of Uranus was investigated by Tripathi and Singhal [3] using an anisotropic kappa loss-cone distribution. By analyzing electron pitch-angle diffusion and energy diffusion coefficients, it was shown that electrons of energy above about 20 keV may be available to precipitate into planetary atmosphere.

In the study of whistler mode waves, it can be assumed that plasma consist of two species of electrons: hot and cold electrons. The hot electrons are responsible for wave amplification or damping and wave propagation is mainly determined by cold electrons with a density well above that of hot electrons [4]. Pandey et al. [5] worked on the effect of cold plasma injection on whistler mode instability separately for a bi-Maxwellian and a loss-cone background plasma with perpendicular AC electric field. They found that it is not the magnitude but the frequency of AC field that influences the growth rate of whistler mode waves in Uranian magnetosphere. It was also shown that loss-cone background plasma had a triggering effect on the growth rate, increasing the value of the real frequency and maximum growth rate by an order of magnitude.

The charged particles in ionosphere and magnetosphere exhibit anisotropic distribution in momentum space, which is suitable for cyclotron instability. This leads to growth in wave, so particle precipitate into the atmosphere. Singh et al. [6] evaluated the effect of thermal velocity of plasma particles on the energy of resonantly interacting energetic electrons with the propagating whistler mode

waves as a function of wave frequency and L-value for the normal and disturbed magnetospheric conditions. It is also observed that some of the instabilities in magnetosphere are 'beam based'. The relativistic electron beam passing through plasma quickly creates a return current and the resulting system exhibits various linear electromagnetic instabilities. Such a system has been studied by Bret et al. [7]. They investigated the effects of both transverse and parallel beam and plasma temperatures on the linear stability of collective electromagnetic modes. Focus was on non relativistic temperatures and wave vector orientations ranging from two-stream to filament instabilities. Water bag distribution was used to model temperature effects and discussed their relevance. Bret et al. [8] systematically worked the electromagnetic instabilities in the whole \mathbf{k} space for a cold relativistic beam interacting with transversely hot plasma. The electrostatic or longitudinal approximation captured only longitudinal modes and therefore failed to recover both Weibel and filamentation instabilities.

Using unperturbed Lorentzian (κ) distribution in Earth's atmosphere, Pandey et al. [9] studied the effect of cold plasma beam on electromagnetic whistler wave for relativistic plasma. Cold plasma was described by a simple Maxwellian distribution. For relativistic back ground plasma, Lorentzian (κ) distribution function was derived with temperature anisotropy in the presence of perpendicular AC electric field to form hot/warm background. The study concluded that along with other factors, relativistic plasma modified the growth rate and it also significantly shifted the wave band. This increase in growth rate and widening of bandwidth explained wide frequency range of whistler emissions in magnetoplasma.

Parallel propagating plasma waves in the vicinity of magnetosphere at very low frequencies have been studied by many workers. Using a series of 1-d simulations, the growth of whistler wave was studied by Zhang et al. [10] from an anisotropic electron beam of various electrostatic and electromagnetic wave modes at various propagation angles. Devine et al. [11] generalized oblique whistler mode instability in one and two dimensional simulation.

The study relevant to the analysis of ion conics in the presence of electromagnetic ion-cyclotron (EMIC) wave in the auroral acceleration region of the magnetoplasma was done by Ahirwar et al. [12]. Following particle aspect approach, the effect of parallel and perpendicular resonant energy and marginal stability of EMIC wave with general loss-cone distribution function in a low β homogeneous plasma has been stressed. It is assumed that resonant particles participate in energy exchange with waves, and non-resonant particles are responsible

for oscillatory motion of the waves. This implies that the effect of parallel electric field with the general distribution function is to control the growth rate of EMIC waves, and the effect of steep loss-cone distribution was to enhance the growth rate and perpendicular heating of the ions.

Various authors have discussed electric field measurement at magnetospheric heights and shock regions giving the values of AC field along and perpendicular to Earth's magnetic field [13–15]. Studies have also been done on the role of parallel AC and DC electric fields on the whistler mode instability in the magnetosphere. The analysis was performed adopting plasma dispersion function which is based on anisotropic Maxwellian distribution to describe resonant population [16, 17].

In the recent past, the instability of field-aligned whistler waves was studied by Pandey and Singh [18], for subtracted bi-Maxwellian magnetoplasma in the presence of perpendicular AC electric field. Using characteristic solution and kinetic approach, it was inferred that, for the generation of whistler mode waves, along with temperature anisotropy, there were other important parameters too.

Motivated from the qualitative investigations done for Uranian magnetosphere and magnetosphere, the present work explains the effect of cold electron beam for Whistler mode waves for relativistic subtracted bi-Maxwellian distribution in the presence of perpendicular AC electric field by using the method of characteristic solutions and kinetic approach. The detailed derivation and calculations has been done for dispersion relation and growth rate for magnetosphere of Uranus. Parametric analysis has been done by changing plasma parameters: thermal velocity, ac frequency, temperature anisotropy, etc.. The effect of AC frequency on the Doppler shifting frequency and comparative study of relativistic and non-relativistic effect on growth rate are analyzed. The new results using subtracted bi-Maxwellian distribution function are found and discussed in connection to a bi-Maxwellian distribution. The comparative study of relativistic and non-relativistic plasma has been done in this paper. It is seen that the effective parameters for the generation of Whistler mode wave are not only the temperature anisotropy but also the relativistic factor, AC field frequency, amplitude of subtracted distribution and width of the loss-cone distribution function which has been discussed in result and discussion section.

2. DISPERSION RELATIONS AND GROWTH RATE

A homogeneous anisotropic collisionless plasma in the presence of an external magnetic field $B_o = B_o \hat{e}_z$ and an electric field $E_{ox} = E_o \sin(vt) \hat{e}_x$ is assumed. In interaction zone in homogeneity is assumed to be small. In order to obtain the particle trajectories perturbed distributions function and dispersion relation, the linearised Vlasov-Maxwell equations are used. Separating the equilibrium and non-equilibrium parts neglecting the higher order terms and following the techniques of Pandey and Singh [18], linearized Vlasov equations are given as:

$$v \cdot \left(\frac{\delta f_0}{\delta r} \right) + \left(\frac{e_s}{m_e} \right) \left[E_0 \sin vt + \frac{(v \times B_0)}{c} \right] \cdot \left(\frac{\delta f_0}{\delta v} \right) = 0 \tag{1}$$

$$\left(\frac{\delta f_1}{\delta t} \right) + v \cdot \left(\frac{\delta f_1}{\delta r} \right) + \left(\frac{F}{M_e} \right) \cdot \left(\frac{\delta f_1}{\delta v} \right) = S(r, v, t) \tag{2}$$

where the force

$$F = e \left[E_0 \sin vt + \frac{(v \times B_0)}{c} \right] = m \frac{dv}{dt} \tag{3}$$

where v is AC frequency and

$$S(r, v, t,) = - \left(\frac{e_s}{m_e} \right) \left[E_1 + \frac{(v \times B_0)}{c} \right] \cdot \left(\frac{\delta f_1}{\delta v} \right) \tag{4}$$

where s denotes the type of electrons. Subscript ‘0’ denotes the equilibrium values. The perturbed distribution function f_1 is determined by using the method of characteristic, which is

$$f_1(r, v, t) = \int_0^\infty S \{ r_0(r, v, t), v_0(r, v, t), t - t' \} dt$$

We have transformed the phase space coordinate system for (r, v, t) to $(r_0, v_0, t - t')$. The relativistic particle trajectories that have been obtained by solving Equation (3) for given external field configuration are

$$X_0 = X + \left(\frac{P_\perp \sin \theta}{\omega_c m_c} \right) - \left[P_\perp \sin \left\{ \frac{\theta + \left(\frac{\omega_c t}{\gamma} \right)}{\omega_c m_c} \right\} \right] + \left[\frac{\Gamma_x \sin vt}{\gamma \left\{ \left(\frac{\omega_c}{\gamma} \right)^2 - v^2 \right\}} \right] - \left[\frac{v \Gamma_x \sin \left(\frac{\omega_c t}{\gamma} \right)}{\omega_c \left\{ \left(\frac{\omega_c}{\gamma} \right) - v^2 \right\}} \right]$$

$$\begin{aligned}
 Y_0 &= Y - \left(\frac{P_{\perp} \cos \theta}{\omega_c m_c} \right) + \left[P_{\perp} \cos \left\{ \frac{\theta + \left(\frac{\omega_c t}{\gamma} \right)}{\omega_c m_c} \right\} \right] \\
 &\quad + \left(\frac{\Gamma_x}{v \omega_c} \right) - \frac{\left\{ 1 + v^2 \beta^2 \cos \left(\frac{\omega_c t}{\gamma} \right) - \omega_c^2 \cos v t \right\}}{\gamma^2 \left\{ \left(\frac{\omega_c}{\gamma} \right)^2 - v^2 \right\}} \\
 z_0 &= z - \frac{P_z}{\beta m_e} \tag{5}
 \end{aligned}$$

and the velocities are

$$\begin{aligned}
 v_{x_0} &= P_{\perp} \cos \left\{ \theta + \frac{\left(\frac{\omega_c t}{\gamma} \right)}{\gamma m_e} \right\} + \left[\frac{v \Gamma_x}{\gamma \left\{ \left(\frac{\omega_c}{\gamma} \right)^2 - v^2 \right\}} \right] \left\{ \cos v t - \cos \left(\frac{\omega_c t}{\gamma} \right) \right\} \\
 v_{y_0} &= P_{\perp} \sin \left\{ \theta + \frac{\left(\frac{\omega_c t}{\gamma} \right)}{\gamma m_e} \right\} + \left[\frac{\Gamma_x}{\gamma \left\{ \left(\frac{\omega_c}{\gamma} \right)^2 - v^2 \right\}} \right] \left\{ \left(\frac{\omega_c}{\gamma} \right) \sin v t - v \sin \left(\frac{\omega_c t}{\gamma} \right) \right\} \\
 v_{z_0} &= \frac{P_z}{\gamma m_e}, \quad v_x = \frac{P_{\perp} \cos \theta}{\gamma m_e}, \quad v_y = \frac{P_{\perp} \sin \theta}{\gamma m_e}, \quad v_z = \frac{P_z}{\gamma m_e} \\
 m_e &= \frac{m_s}{\gamma}, \quad \omega_c = \frac{e B_0}{m_e}, \quad \gamma = \sqrt{1 - \frac{v^2}{c^2}}, \quad \Gamma_x = \frac{e E_0}{m_e} \tag{6}
 \end{aligned}$$

P_{\perp} and P_z denote momenta perpendicular and parallel to the magnetic field. Using Equations (5), (6) and the Bessel identity and performing the time integration, following the technique and method of Pandey and Singh [18, 19], the perturbed distribution function is found after some lengthy algebraic simplifications as:

$$\begin{aligned}
 f_1 &= - \left(\frac{i e_s}{m \gamma \omega} \right) \sum J_s(\lambda_3) \exp i(m - n)\theta \\
 &\quad \left[\frac{J_m J_n J_p U * E_{1x} - i J_m V * E_{1y} + J_m J_n J_p W *}{\omega - \left(\frac{k_{\parallel} P_z}{\gamma m_e} + p v - \frac{(n+g)\omega_c}{\gamma} \right)} \right] \tag{7}
 \end{aligned}$$

Due to the phase factor the solution is possible when $m = n$. Here

$$U^* = \left(\frac{c_1 P_{\perp} n}{\gamma \lambda_1 m_e} \right) - \left(\frac{n v c_1 D}{\lambda_1} \right) + \left(\frac{p v c_1 D}{\lambda_2} \right),$$

$$\begin{aligned}
 V^* &= \left(\frac{c_1 P_\perp J_n J_p}{\gamma m_e} \right) + c_1 D J_p J_n \omega_c \\
 W^* &= \left(\frac{n \omega_c F m_e}{k_\perp P_\perp} \right) + \left(\frac{\gamma m_e P_\perp \omega \partial f_0}{\partial P_z} \right) + G \left\{ \left(\frac{p}{\lambda_2} \right) - \left(\frac{n}{\lambda_1} \right) \right\} \\
 C_1 &= \left\{ \frac{(\gamma m_e)}{P_\perp} \right\} \left(\frac{\partial f_0}{\partial P_\perp} \right) \left(\omega - \frac{k_\parallel p_z}{\gamma m_e} \right) + k_\parallel \gamma m_e \left(\frac{\partial f_0}{\partial P_\perp} \right) \\
 D &= \left[\frac{\Gamma_x}{\gamma \left\{ \left(\frac{\omega_c}{\gamma} \right)^2 - v^2 \right\}} \right], \quad F = \frac{H k_\perp P_\perp}{\gamma m_e}, \\
 H &= \left\{ \frac{(\gamma m_e)^2}{P_\perp} \right\} \left(\frac{\partial f_0}{\partial P_\perp} \right) \left(\frac{P_z}{\gamma m_e} \right) + \gamma m_e \left(\frac{\partial f_0}{\partial P_z} \right) \\
 G &= \frac{H k_\perp v \Gamma_x}{\gamma \left\{ \left(\frac{\omega_c}{\gamma} \right)^2 - v^2 \right\}}, \quad J_n(\lambda_1) = \frac{dJ_n(\lambda_1)}{d\lambda_1}, \quad J_p(\lambda_2) = \frac{dJ_p(\lambda_2)}{d\lambda_2}
 \end{aligned}$$

and the Bessel function arguments are defined as

$$\lambda_1 = \frac{k_\perp P_\perp}{\omega_c m_e} \lambda_2 = \frac{k_\perp \Gamma_x}{\gamma \left\{ \left(\frac{\omega_c}{\gamma} \right)^2 - v^2 \right\}}, \quad \lambda_3 = \frac{k_\perp v \Gamma_x}{\gamma \left\{ \left(\frac{\omega_c}{\gamma} \right)^2 - v^2 \right\}}$$

The conductivity tensor $\|\sigma\|$ is found to be

$$\|\sigma\| = \frac{-i \sum (e^2 / \gamma m_e)^2 \omega \int d^3 P J_g(\lambda_3) \|s\|}{\left[\omega - \left(\frac{k_\parallel P_z}{\gamma m_e} \right) - \left((n+g) \frac{\omega_c}{\gamma} \right) + pv \right]}$$

where

$$\|S\| = \begin{vmatrix} P_\perp J_n^2 J_p \left(\frac{n}{\lambda_1} \right) U^* & iP_\perp J_n V^* & P_\perp J_n^2 J_p \left(\frac{n}{\lambda_1} \right) W^* \\ P_\perp J_n J_n J_p \left(\frac{n}{\lambda_1} \right) U^* & iP_\perp J_n V^* & P_\perp J_n J_n J_p \left(\frac{n}{\lambda_1} \right) W^* \\ P_z J_n^2 J_p \left(\frac{n}{\lambda_1} \right) U^* & iP_z J_n V^* & P_z J_n^2 J_p \left(\frac{n}{\lambda_1} \right) W^* \end{vmatrix}$$

By using these in the Maxwell's equations we get the dielectric tensor,

$$\epsilon_{ij} = 1 + \sum \left\{ \frac{4\pi e_s^2}{(\gamma m_e)^2 \omega} \right\} \int \frac{d^3 P J_g(\lambda_3) \|S\|}{\left(\omega - \frac{k_\parallel P_z}{\gamma m_e} \right) - \left\{ \frac{(n+g)\omega_c}{\gamma} \right\} + pv}. \quad (8)$$

For parallel propagating whistler mode instability, the general dispersion relation reduces to

$$\epsilon_{11} \pm E_{12} = N^2, \quad N^2 = \frac{k^2 c^2}{\omega^2}$$

The dispersion relation for relativistic case with perpendicular AC electric field for $g = o$, $p = 1$, $n = 1$ is written as:

$$\frac{k^2 c^2}{\omega^2} = 1 + \frac{4\pi e_s^2}{(\gamma m_e)^2 \omega^2} \int \frac{d^3 P}{\gamma} \left[\frac{P_\perp}{2} - \frac{v \Gamma_x m_e}{2 \left(\frac{\omega_c^2}{\gamma^2} - v^2 \right)} \right] \left[\left(\gamma \omega - \frac{k_{\parallel} P_{\parallel}}{m_e} \right) \frac{\partial f_0}{\partial P_\perp} + \frac{P_\perp k_{\parallel}}{m_e} \frac{\partial f_0}{\partial P_{\parallel}} \right] \frac{1}{\gamma \omega - \frac{k_{\parallel} P_{\parallel}}{m_e} - \omega_c + \gamma v} \quad (9)$$

The subtracted bi-Maxwellian distribution function is given as

$$f_0 = \frac{n_0}{\pi^{3/2} p_{0\perp}^2 p_{0\parallel}} \left[\left\{ \left(1 + \frac{\beta \delta}{1 - \beta} \right) \exp - \left(\frac{p_\perp^2}{p_{0\perp}^2} \right) - \frac{\delta}{1 - \beta} \exp - \left(\frac{p_\perp^2}{\beta p_{0\perp}^2} \right) \right\} \exp - \left(\frac{p_{0\parallel}}{p_{0\parallel}^2} \right)^2 \right] \quad (10)$$

where p_\perp and p_{\parallel} are perpendicular and parallel moment a for a temperature T. Substituting and using Equations (9), (10) and doing integration by parts the dispersion relation is found as,

$$D(k, \omega) = 1 + \frac{\omega_{ps}^2}{\lambda \omega^2} \sum J_p(\alpha_2) J_g(\alpha_3) \left[(1 - X_1) \left(\frac{\lambda m_e \omega - k_{\parallel} p_{\parallel}}{k_{\parallel} p_{0\parallel}} \right) Z(\xi) + (A_T + X_2 - X_1) (1 + \xi Z(\xi)) \right] - \frac{\omega_{pc}^2}{\omega^2} \frac{1}{\omega \pm \omega_c} \quad (11)$$

where

$$\begin{aligned} X_1 &= \frac{v \Gamma_x \lambda m_e}{2 \lambda \left(\left(\frac{\omega_c}{\lambda} \right)^2 - v^2 \right)} \frac{1}{p_{0\perp}} \left[\left(1 + \frac{\beta \delta}{1 - \beta} \right) - \frac{\delta \sqrt{\beta}}{1 - \beta} \right] \\ X_2 &= \frac{v \Gamma_x \lambda m_e}{2 \lambda \left(\left(\frac{\omega_c}{\lambda} \right)^2 - v^2 \right)} \frac{p_{0\perp}}{p_{0\parallel}^2} \left[\left(1 + \frac{\beta \delta}{1 - \beta} \right) - \frac{\beta^{3/2} \delta}{1 - \beta} \right] \\ A_T &= \frac{p_{0\perp}^2}{p_{0\parallel}^2} \left[\left(1 + \frac{\beta \delta}{1 - \beta} \right) - \frac{\beta^2 \delta}{1 - \beta} \right] - 1, \\ p_{0\perp} &= \left(\frac{k_B T_\perp}{m_e} \right)^{1/2}, \quad p_{0\parallel} = \left(\frac{k_B T_{\parallel}}{m_e} \right)^{1/2} \\ \omega_{he}^2 &= \frac{4\pi \pi_s^2 n_{he}}{m_e}, \quad \omega_{pe}^2 = \frac{4\pi \pi_s^2 n_{pe}}{m_e} \end{aligned} \quad (12)$$

$P_{0\parallel}$ and P_0 are respective thermal speeds parallel and perpendicular to the background magnetic field.

$$\xi = \frac{\lambda m_e \omega \pm m_e \omega_c - m_e g \omega_c + \lambda m_e p v}{k_{\parallel} p_{0\parallel}} \quad (13)$$

For real k and substituting $\frac{k^2 c^2}{\omega^2} \gg 1$.

The expression for growth rate for real frequency ω_r in dimensionless form is found to be

$$\frac{\gamma}{\omega_c} = \frac{\frac{\sqrt{\pi}}{\tilde{k}}(k_1 - k_3)k_4^3 \exp\left\{-\left(\frac{k_4}{\tilde{k}}\right)\right\}^2}{1 + \lambda X_4 + \frac{\tilde{k}^2(1 + \lambda X_4)}{2k_4^2} - \frac{\tilde{k}^2}{k_4}(k_1 - k_3) + \frac{(\delta_1 - 1)k_4^2}{(1 - \lambda X_3)^2(1 + \lambda X_4)}} \quad (14)$$

$$X_3 = \frac{\tilde{k}^2}{\beta_1 \delta_1} \left[k_2(1 + \lambda X_4) + k_1 \frac{\beta_1}{2(1 + \lambda X_4)} \right] \quad (15)$$

where

$$\begin{aligned} k_3 &= \frac{\lambda X_3}{1 - \lambda X_3 + \lambda X_4}, \quad \tilde{k} = \frac{k_{||} p_{0||}}{m_e \omega_c}, \quad k_4 = 1 - \lambda X_3 + \lambda X_4, \\ X_3 &= \frac{\omega_r}{\omega_c}, \quad X_4 = \frac{-\lambda v}{\omega_c}, \quad \beta_1 = \frac{k_B T_{||} \mu_0 n_0}{B_0^2}, \\ k_1 &= \frac{A_T + X_2 - X_1}{1 - X_1}, \quad k_2 = \frac{p_{0\perp}^2}{2}, \quad \delta_1 = 1 + \frac{n_c}{n_w} k_2 (1 + \lambda X_4) \end{aligned} \quad (16)$$

3. RESULTS AND DISCUSSION

Following plasma parameters have been adopted for the calculation of the growth rate for the loss-cone driven whistler instability in Uranian magnetosphere. Ambient magnet field $B_o = 2.4 \times 10^{-10}$ T, electron density $n_o = 5 \times 10^4 \text{ m}^3$ and magnitude of AC electric field $E_o = 4 \text{ mV/m}$ has been considered. Temperature anisotropy A_T is supposed to vary from 1.25 to 1.75 and density ratio n_c/n_w is to vary from 10 to 30. Width and amplitude of loss-cone distribution function are taken to be 0.7, 0.8, 0.9 and 0.5, 0.6, 0.7 respectively. Also AC frequency varies from 6 Hz to 18 Hz. For relativistic study $\gamma = 0.5$ and for non-relativistic analysis $\gamma = 1$.

Figure 1(a) shows the variation of relativistic dimensionless Growth Rate with respect to \tilde{k} for various values of ratio of perpendicular to parallel temperature $T_{\perp}/T_{||}$ and other fixed parameters as listed in figure caption. For $T_{\perp}/T_{||} = 1.25$ the peak value appears at $\tilde{k} = 1$ and growth rate $\gamma/\omega_c = 0.029$ and for $T_{\perp}/T_{||} = 1.50$, peak value comes at $\tilde{k} = 0.9$ and $\gamma/\omega_c = 0.039$. As ratio of perpendicular to parallel temperature $T_{\perp}/T_{||}$ increases to 1.75, peak shifts to lower value $\tilde{k} = 0.8$ and $\gamma/\omega_c = 0.042$. Since it is seen that growth rate increases with increasing value of perpendicular to parallel temperature ratio $T_{\perp}/T_{||}$, it can be said temperature anisotropy $A_T = T_{\perp}/T_{||} - 1$ is free energy source. Also bandwidth did change and

maxima changes for lower value of \tilde{k} . Thus we may conclude that in this case the injection of electron particles have a positive slope in v_{\perp} . Fig. 1(b) shows the variation of non-relativistic dimensionless Growth Rate with respect to \tilde{k} for various values of ratio of perpendicular to parallel temperature. For $T_{\perp}/T_{\parallel} = 1.25$ the peak is seen at $\tilde{k} = 1.1$ and growth rate $\gamma/\omega_c = 0.010$ and for $T_{\perp}/T_{\parallel} = 1.50$, peak value is at $\tilde{k} = 1$ and $\gamma/\omega_c = 0.014$. For $T_{\perp}/T_{\parallel} = 1.75$, peak appears at $\tilde{k} = 0.9$ and $\gamma/\omega_c = 0.017$. Comparing the results of Fig. 1(a) with that of Fig. 1(b), it is observed that order of growth of whistler mode wave is more in relativistic case than in non-relativistic case in relativistic case particles of background plasma have high energy.

Figure 2(a) shows the variation of relativistic dimensionless Growth Rate with respect to \tilde{k} for various values of density ratio n_c/n_w at other plasma parameters being fixed and listed in caption. The figure shows that for different values of n_c/n_w the peak value appears at wave number $\tilde{k} = 0.9$. For $n_c/n_w = 10, 20$ and 30 , growth rate is $\gamma/\omega_c = 0.027, 0.014, 0.009$ respectively. It is seen that growth rate decreases with increasing value of ratio of cold beam particles to hot beam particles n_c/n_w by increasing the cold electron the whistler mode wave transmits more energy to cold plasma particles during their interaction. It indicates that the injected cold electron is not decaying to zero value through loss from the field aligned density gradient of the magnetosphere of Uranus. Fig. 2(b) shows the variation of non-

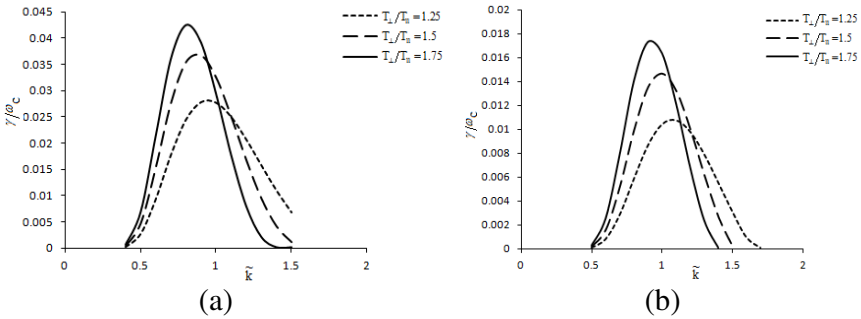


Figure 1. (a) Variation of relativistic Growth Rate with respect to \tilde{k} for various values of T_{\perp}/T_{\parallel} at other plasma parameters being $B_o = 2.4 \times 10^{-10}$ T, $E_o = 4$ mV/m, $K_B T_{\parallel} = 10$ eV, $\beta = 0.7$, $\delta = 0.5$, $\gamma = 0.5$, $n_c/n_w = 10$ and $v = 18$ Hz. (b) Variation of non-relativistic Growth Rate with respect to \tilde{k} for various values of T_{\perp}/T_{\parallel} at other plasma parameters being $B_o = 2.4 \times 10^{-10}$ T, $E_o = 4$ mV/m, $K_B T_{\parallel} = 10$ eV, $\beta = 0.7$, $\delta = 0.5$, $\gamma = 1$, $n_c/n_w = 10$ and $v = 18$ Hz.

relativistic dimensionless Growth Rate with respect to \tilde{k} for various values of n_c/n_w . In this figure, for $n_c/n_w = 10, 20$ and 30 , peak values occur at $\tilde{k} = 1.1$ growth rate being $\gamma/\omega_c = 0.010, 0.005, 0.003$ respectively. Comparing Fig. 2(a) with that of Fig. 2(b) it is inferred that although order of growth of whistler mode wave is more in relativistic case than in non-relativistic case but in non-relativistic case, peak value of growth rate appears at higher wave number than in relativistic case.

Figure 3(a) shows the variation of relativistic dimensionless Growth Rate with respect to \tilde{k} for various values of AC frequency v at other plasma parameters being fixed and listed in figure caption. For $v = 6$ Hz the peak value is observed at $\tilde{k} = 0.9$ and growth rate $\gamma/\omega_c = 0.0289$ and for $v = 12$ Hz, peak value comes at $\tilde{k} = 0.9$ and $\gamma/\omega_c = 0.0285$. And as v increases to 18 Hz, peak can be seen at $\tilde{k} = 0.9$ and $\gamma/\omega_c = 0.0278$. This implies that introducing the AC signal increases the growth rate and the bandwidth. As increase of AC frequency increases the growth rate due to negative exponential of Landau damping, this effect of increasing bandwidth with increasing AC field increases. AC frequency has a triggering effect on the growth rate. The Landau damping or instability is mainly caused due to exchange of energy among electron and component of the wave electric field parallel to external magnetic field. Also it can be seen that Doppler shift in frequency is not affected by the magnitude of the

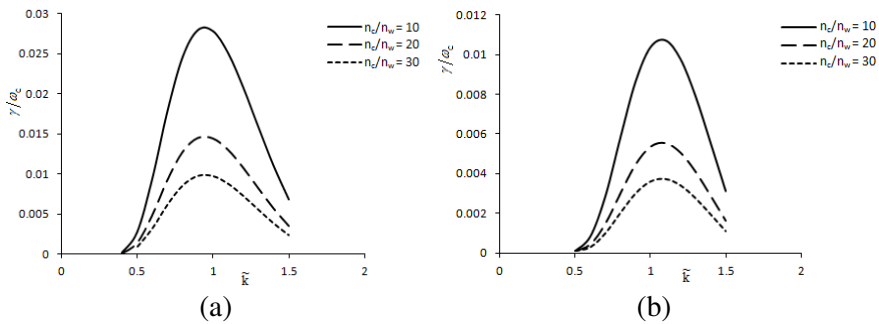


Figure 2. (a) Variation of relativistic Growth Rate with respect to \tilde{k} for various values of ratio of n_c/n_w at other plasma parameters being $B_o = 2.4 \times 10^{-10}$ T, $E_o = 4$ mV/m, $K_B T_{||} = 10$ eV, $\beta = 0.7$, $\delta = 0.5$, $\gamma = 0.5$, $T_{\perp}/T_{||} = 1.25$ and $v = 18$ Hz. (b) Variation of non-relativistic Growth Rate with respect to \tilde{k} for various values of n_c/n_w at other plasma parameters being $B_o = 2.4 \times 10^{-10}$ T, $E_o = 4$ mV/m, $K_B T_{||} = 10$ eV, $\beta = 0.7$, $\delta = 0.5$, $\gamma = 1$, $T_{\perp}/T_{||} = 1.25$ and $v = 18$ Hz.

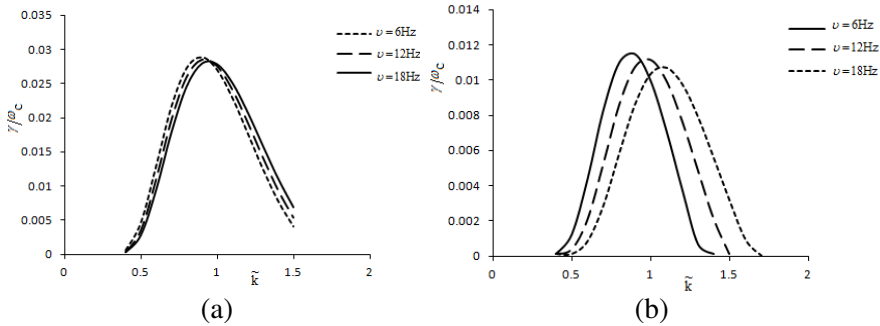


Figure 3. (a) Variation of relativistic Growth Rate with respect to \tilde{k} for various values of AC frequency ν at other plasma parameters being $B_o = 2.4 \times 10^{-10}$ T, $E_o = 4$ mV/m, $K_B T_{ll} = 10$ eV, $\beta = 0.7$, $\delta = 0.5$, $\gamma = 0.5$, $n_c/n_h = 10$ and $T_{\perp}/T_{ll} = 1.25$. (b) Variation of relativistic Growth Rate with respect to \tilde{k} for various values of AC frequency ν at other plasma parameters being $B_o = 2.4 \times 10^{-10}$ T, $E_o = 4$ mV/m, $K_B T_{ll} = 10$ eV, $\beta = 0.7$, $\delta = 0.5$, $\gamma = 1$, $n_c/n_h = 10$ and $T_{\perp}/T_{ll} = 1.25$.

electric field, but only by its frequency. Fig. 3(b) shows the variation of non-relativistic dimensionless Growth Rate with respect to \tilde{k} for various values of AC electric field frequency. For $\nu = 6$ Hz the peak appears at $\tilde{k} = 1.1$ and growth rate $\gamma/\omega_c = 0.010$ and for $\nu = 12$ Hz, peak value is at $\tilde{k} = 1$ and $\gamma/\omega_c = 0.014$. For $\nu = 18$ Hz, peak shifts to lower value of \tilde{k} at 0.9 and $\gamma/\omega_c = 0.017$. Comparative study of Fig. 3(a) and Fig. 3(b) reveals that order of growth of whistler mode wave is more in relativistic case than in non-relativistic case. It means that the subtracted distribution is more suitable in case of relativistic rather than non-relativistic.

Figure 4(a) shows the variation of relativistic dimensionless Growth Rate with respect to \tilde{k} for various values of width of loss-cone distribution function β at other plasma parameters being fixed and listed in the figure caption. The figure shows that for different values of β the peak value of dimensionless growth rate appears at wave number $\tilde{k} = 0.9$. For $\beta = 0.7, 0.8$ and 0.9 , growth rate is $\gamma/\omega_c = 0.027, 0.028, 0.029$, respectively. It is seen that growth rate increases with increasing value of β . Mathematically if $\beta \geq 1$ then the factor $\delta/1 - \beta$ is infinite or negative. Fig. 4(b) shows the variation of non-relativistic dimensionless Growth Rate with respect to \tilde{k} for various values of width of loss-cone distribution function β . The figure explains that for $\beta = 0.7, 0.8$ and 0.9 , peak values occur at

$\tilde{k} = 1$. For different widths of loss-cone distribution function, the peak value remains same but growth rate varies slightly, i.e., $\gamma/\omega_c = 0.0103, 0.0108, 0.011$ respectively. Comparison between Fig. 4(a) and Fig. 4(b) show that although order of growth of whistler mode wave is larger in relativistic case than in non-relativistic case but in non-relativistic case, peak value of growth rate appears at higher wave number than in relativistic case.

Figure 5(a) shows the variation of relativistic dimensionless Growth Rate with respect to \tilde{k} for various values of amplitude of loss-cone distribution function δ at other plasma parameters being fixed and stated in figure caption. For $\delta = 0.5, 0.6$ and 0.7 , the peak value of growth rate appears at wave number $\tilde{k} = 0.9$ for different values of δ and growth rate is $\gamma/\omega_c = 0.027, 0.029, 0.031$ respectively. It is seen that growth rate increases with increasing value of ratio of β . Fig. 5(b) shows the variation of non-relativistic dimensionless Growth Rate with respect to \tilde{k} for various values of amplitude of loss-cone distribution function δ . The figure explains that for $\delta = 0.5, 0.6$ and 0.7 , peak values occur at $\tilde{k} = 1.1$ where growth rate is $\gamma/\omega_c = 0.010, 0.011, 0.012$ respectively. Comparing Fig. 5(a) with that of Fig. 5(b) shows that although order of growth of whistler mode wave is larger in relativistic case than in non-relativistic case but in non-relativistic case, peak value of growth rate appears at higher wave number than in relativistic case.

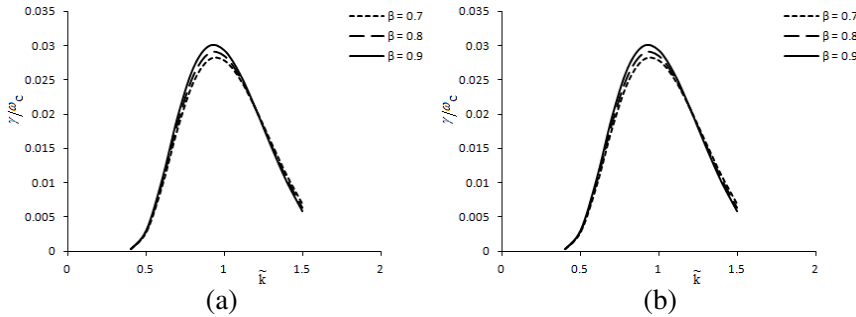


Figure 4. (a) Variation of relativistic Growth Rate with respect to \tilde{k} for various values of β at other plasma parameters being $B_o = 2.4 \times 10^{-10}$ T, $E_o = 4$ mV/m, $K_B T_{ll} = 10$ eV, $\nu = 18$ Hz, $\delta = 0.5$, $\gamma = 0.5$, $n_c/n_w = 10$ and $T_{\perp}/T_{ll} = 1.25$. (b) Variation of non-relativistic Growth Rate with respect to \tilde{k} for various values of β at other plasma parameters being $B_o = 2.4 \times 10^{-10}$ T, $E_o = 4$ mV/m, $K_B T_{ll} = 10$ eV, $\nu = 18$ Hz, $\delta = 0.5$, $\gamma = 1$, $n_c/n_w = 10$ and $T_{\perp}/T_{ll} = 1.25$.

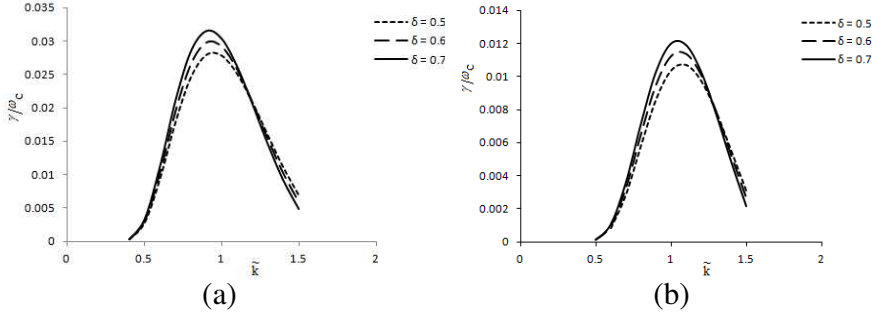


Figure 5. (a) Variation of relativistic Growth Rate with respect to \tilde{k} for various values of δ at other plasma parameters being $B_o = 2.4 \times 10^{-10}$ T, $E_o = 4$ mV/m, $K_B T_{ll} = 10$ eV, $\beta = 0.7$, $\delta = 0.5$, $\gamma = 0.5$, $n_c/n_h = 10$ and $T_{\perp}/T_{ll} = 1.25$. (b) Variation of non-relativistic Growth Rate with respect to \tilde{k} for various values of δ at other plasma parameters being $B_o = 2.4 \times 10^{-10}$ T, $E_o = 4$ mV/m, $K_B T_{ll} = 10$ eV, $\beta = 0.7$, $\delta = 0.5$, $\gamma = 1$, $n_c/n_h = 10$ and $T_{\perp}/T_{ll} = 1.25$.

4. CONCLUSION

It is concluded from the above illustrations that the growth rate increases with increasing value of perpendicular to parallel temperature ratio implying that temperature anisotropy is free energy source. Since maxima changes for lower value of \tilde{k} it can be said that injection of electron particles have a positive slope in v_{\perp} . It is noticed that growth rate decreases with increasing value of ratio of cold beam particles to hot beam particles n_c/n_w . By increasing the cold electron the whistler mode wave transmits more energy to cold plasma particles during their interaction. The existence of such a situation may give rise to emissions over a broad frequency range and can be used to explain the entire frequency spectrum of VLF emissions. Introduction of AC signal increases the growth rate and the bandwidth. As increase of AC frequency increases the growth rate due to negative exponential of Landau damping, this effect of increasing bandwidth with increasing AC field increases. AC frequency has a triggering effect on the growth rate. Also it can be seen that Doppler shift in frequency is not affected by the magnitude of the electric field, but only by its frequency. Growth rate is also affected by the value of amplitude and width of loss-cone distribution function. It increases as the value of δ and β increases. Comparative study of relativistic and non-relativistic cases reveals that order of growth of whistler mode wave is

larger in relativistic case than in non-relativistic case whenever there is increase in perpendicular to parallel temperature ratio, AC frequency, amplitude and width of loss-cone distribution function. It means that the subtracted distribution is more suitable in case of relativistic rather than non-relativistic.

REFERENCES

1. Gurnett, D. A., W. S. Kurth, F. L. Scarf, and R. L. Poynter, "First plasma wave observations at Uranus," *Science*, Vol. 233, 106–109, 1986.
2. Kurth, W. S., "Voyager plasma wave observations near the outer planets," *Adv. Space Res.*, Vol. 11, 59–68, 1991.
3. Tripathi, A. K. and R. P. Singhal, "Whistler mode instability in magnetosphere of Uranus and Neptune," *Planet Space Sci.*, Vol. 56, 310–319, 2007.
4. Sazhin, S. S. and N. M. Temme, "Marginal stability of parallel whistler mode wave (Asymptotic Analysis)," *Ann. Geophysicae*, Vol. 9, 304, 1991.
5. Pandey, R. P., S. M. D. Karim, and K. M. Singh, "Effect of cold plasma injection on whistler mode instability triggered by perpendicular AC electric field at Uranus," *Earth, Moon and Planets*, Vol. 91, 195–207, 2002.
6. Singh, D., S. Singh, and R. P. Singh, "Thermal effects on parallel resonance energy of whistler mode wave," *Pramana — J. Phys.*, Vol. 66, 467–472, 2006.
7. Bret, A., M.-C. Firpo, and C. Deutsch, "Electromagnetic instabilities for relativistic beam-plasma interaction in whole k space: Nonrelativistic beam and temperature effects," *Physical Review E*, Vol. 72, 016403–016403.14, 2005.
8. Bret, A., M.-C. Firpo, and C. Deutsch, "Collective electromagnetic modes for beam-plasma interaction in the whole k space," *Physical Review E*, Vol. 70, 046401, 2004.
9. Pandey, R. S., R. P. Pandey, K. M. Singh, and N. M. Mishra, "Cold plasma injection on VLF wave mode for relativistic magnetoplasma with AC electric field," *Progress In Electromagnetic Research C*, Vol. 2, 217–232, 2008.
10. Zhang, Y. L., H. Matsumoto, and Y. Omura, "Linear and nonlinear interactions of an electron beam with oblique whistler and electrostatic waves in the magnetosphere," *J. Geophys. Res.*, Vol. 98, 21353, 1993.

11. Devine, P. E., S. C. Chapman, and J. W. Eastwood, "One- and two-dimensional simulations of whistler mode waves in an anisotropic plasma," *J. Geophys. Res.*, Vol. 100, 17189–17203, 1995.
12. Ahirwar, G., P. Varma, and M. S. Tiwari, "Electromagnetic ion-cyclotron instability in the presence of a parallel electric field with general loss-cone distribution function — Particle aspect analysis," *Ann. Geophysicae*, Vol. 24, 1919–1930, 2006.
13. Mozer, F. S., R. B. Torbert, U. V. Fahlson, C. Falthammar, A. Gonafalone, A. Pedersen, and C. T. Russel, "Electric field measurements in the solar wind bow shock, magnetosheath, magnetopause and magnetosphere," *Space Sci. Rev.*, Vol. 22, 791, 1978.
14. Wygant, J. R., M. Bensadoun, and F. S. Mozer, "Electric field measurements at sub critical, oblique bow shock crossings," *J. Geophys. Res.*, Vol. 92, 11109, 1987.
15. Lindquist, P. A. and F. S. Mozer, "The average tangential electric field at the noon magnetopause," *J. Geophys. Res.*, Vol. 95, 17137, 1990.
16. Misra, K. D. and R. S. Pandey, "Generation of whistler emissions by injection of hot electrons in the presence of perpendicular AC electric field," *J. Geophys. Res.*, Vol. 100, 19405, 1995.
17. Misra, K. D. and B. D. Singh, "On the modification of whistler mode instability in the magnetopause in the presence of parallel electric field by cold plasma injection," *J. Geophys. Res.*, Vol. 85, 5138, 1980.
18. Pandey, R. S. and D. K. Singh, "Whistler mode instability with AC electric field for relativistic subtracted bi-maxwellian magneto-plasma," *Archives of Applied Sci. Res.*, Vol. 3, No. 5, 350–361, 2011.
19. Pandey, R. S. and D. K. Singh, "Study of electromagnetic ion cyclotron instability in magneto-plasma," *Progress In Electromagnetic Research M*, Vol. 14, 147–161, 2010.